Proceedings of IMECE2007
2007 ASME International Mechanical Engineering Congress and Exposition
November 11-15, 2007, Seattle, Washington, USA

IMECE2007-41105

CAPSTAN DESIGN AND CONTROL FOR DRAWING OPTICAL FIBER: A CASE STUDY IN MECHATRONICS DESIGN

Hodge E. Jenkins
Dept. of Mechanical and Industrial Engineering
Mercer University
1400 Coleman Ave.
Macon, GA 31207 USA
jenkins_he@mercer.edu

Mark L. Nagurka
Dept. of Mechanical Engineering
Marquette University
P.O. Box 1881
Milwaukee, WI 53201 -1881 USA
mark.nagurka@marquette.edu

ABSTRACT

This paper presents a case study on the design of a draw capstan drive with feedback control for use in optical fiber manufacturing. Optical fiber is manufactured by the draw process, which involves heating and pulling high purity glass cylinders to diameters of 125 micron. Of critical concern is producing a constant diameter for the glass fiber and its light-guide core. The diameter of the optical fiber must remain constant to create a product capable of transmitting high-bandwidth optical data. The optical fiber draw capstan design has a significant impact on the resulting fiber quality. As the draw speed is used to control the fiber diameter, the ability of the draw capstan to follow velocity commands directly affects the resulting fiber diameter.

In this case study a systems approach is used for the design of the mechanical and control aspects through parametric evaluations and modeling, as well as simulation studies of the capstan drive. Disturbances in the draw process arise from sources such as the variation in the diameter of the input glass cylinder and the draw tension control, affecting the glass temperature and viscosity. Simulation studies demonstrate that speed regulation, to manufacture optical fiber within allowable diameter tolerances, is achievable in the presence of representative disturbances.

The capstan model and design along with the fiber-drawing process model presented in this case study are suitable for undergraduate and graduate courses in system dynamics, control, and mechatronics. As is typical of many problems in manufacturing processes, the problem discussed is multi-disciplinary. The study highlights the use of mechanical and electrical modeling, system identification, and control design as necessary parts of product and process improvement.

NOMENCLATURE

B	rotational damping
d	fiber diameter
I	motor current
J	polar mass moment of inertia
K_i	integral gain
K_p	proportional gain
K_t	motor torque constant
M	mass
Q	volumetric flow rate
r	outside radius of capstan pulley
t	time
τ	thickness of capstan pulley rim
v	belt speed ($\omega \times r$)
ω	motor rotational speed
$\dot{\omega}$	motor rotational acceleration
$\Omega(s)$	Laplace transform of $\omega(t)$

INTRODUCTION

Industrial case studies of successful implementations of combined mechanical and closed-loop control designs provide students with meaningful, real-life examples that demonstrate classroom theory. The case study of this paper – the design and control of an optical fiber draw capstan – offers modeling and design challenges that make it highly suitable for teaching undergraduate and graduate students in courses such as system dynamics, controls, and mechatronics. The study exposes

students to system models, practical mechanical design, motor selection, and closed-loop control system design. It highlights how design and performance are linked and can be improved through an integrated, systems-level understanding predicated on engineering fundamentals and tools from multiple technical disciplines.

In industry and too often in academia, the boundaries and barriers between engineering disciplines can be significant. An objective of this case study is to broaden the perspective, and help reduce boundaries – artificial or real – by encouraging a blended problem-solving approach that draws upon several areas of technical knowledge and competence. The design problem here is solved with knowledge and tools from mechanical, electrical, and control engineering.

Drawing upon multiple backgrounds is not a unique approach to solving design problems. There are many similar types of design challenges in industrial applications, and they can be viewed as mechatronic designs. Other real-life examples of mechatronic designs include auto-focus cameras, CD players, smart toasters, and high-tech toys. In general, machines and processes that rely on sensors, actuators, mechanisms, instrumentation, controllers and micro-processors of various types, sizes, and attributes can be called mechatronic systems. It could be said that large-scale systems, such as industrial plants or vehicles, with many control loops and inter-connections under computer control are at one end of the mechatronic spectrum and relatively simpler devices such as magnetic bearings are at the other extreme [1, 2, 3].

DRAW PROCESS BACKGROUND

Optical fiber is a light guide providing high-speed data transmission at the terabit (10^{12}) per second level [4]. Moving light through the glass fiber core relies upon the principle of total internal reflection, where the inside glass core has a higher refractive index than the cladding glass around the core, as shown in Figure 1.

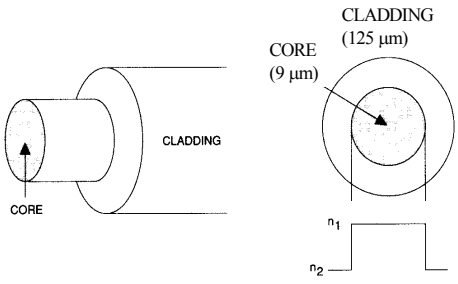

Figure 1. Typical glass components of optical fiber

Optical fiber is manufactured by the draw process. This process is the only cost-effective means of creating optical fiber from ultra-high purity glass cylinders with the required refractive index profile [4, 5, 6]. An important manufacturing quality concern is maintaining a constant core diameter for efficient light transmission. Core geometry variations lead to dispersion of light and loss of signal strength.

Figure 2 illustrates the draw manufacturing process for optical fiber. A high purity glass cylinder with a prescribed optical index profile, known as a 'preform,' is heated in a specially designed furnace to the point where the glass flows under low pulling tension. The draw capstan pulls the fiber from the bottom of the glass preform in the furnace; the glass preform feed drive above the furnace maintains material flow equilibrium through the furnace. The fiber is then cooled, coated with protective polymers, cured under ultraviolet lights, and wound onto spools.

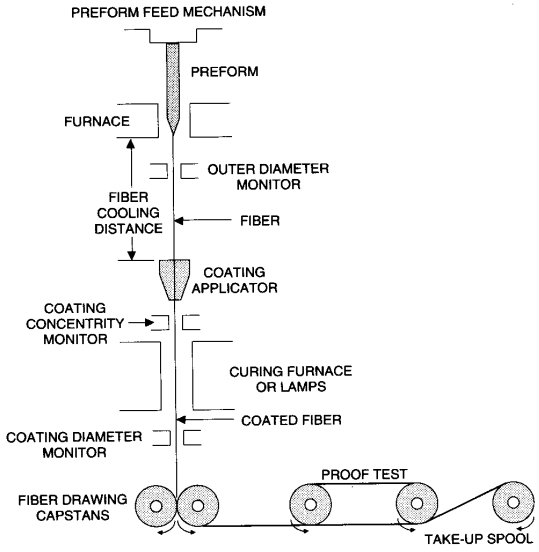

Figure 2. Draw manufacturing process for optical fiber

The capstan controls the diameter of the fiber by adjusting the speed at which the fiber is drawn. Measurement of the input glass diameter occurs just below the furnace. (Cooling occurs rapidly in the thin fiber, so thermal expansion of the fiber relative to room temperature is inconsequential.) The capstan relies on the draw speed to control the diameter. Based on the diameter error about a set point, the capstan's speed is increased when the fiber is too thick and the speed is decreased when the fiber is too thin. (The temperature of the furnace affects the pulling tension placed in the fiber by the capstan. While the pulling tension of the fiber is important in the draw process, it is not discussed in this paper.)

The basic design of the fiber draw capstan is a flexible belt partially wound over a flat pulley that moves/pulls a continuous optical fiber all the way from the heated preform, as shown in Figure 3. Tests have validated a relationship between the fiber diameter and the line speed about an operating point. The basis of the relationship is constant volumetric flow rate of glass.

Variations in fiber diameter arise quite often from process disturbances, such as non-uniformity of the preform diameter, mismatches of the preform feed volumetric flow relative to that of the draw, and drifts in the furnace/glass temperature. Thus, in addition to the mechanical design and motor selection, a speed controller must be incorporated into the capstan design to prevent impermissible variations in the fiber diameter from process disturbances.

Figure 3. Optical fiber drawn by capstan

DESIGN SPECIFICATIONS AND PARAMETERS

The target dimensions of the optical fiber glass are an outside diameter of 125 µm and an inside core diameter of 9 µm. Product specifications call for outside diameter tolerances of ±1 µm. To achieve this specification, the permissible diameter error must be targeted to a lower dimension. Typically, the permissible diameter design deviation is ± 0.1 µm. The capstan mechanical, electrical, and control designs synergistically impact the ability to achieve this fiber diameter tolerance.

With the permissible deviations specified, the next step is to understand how the selected parameters of the capstan design affect the resulting product. While many decisions must be made in any design, there are usually a limited number of critical parameters that have significant influence on operational performance. These parameters include:

- The diameter and tolerances of the capstan pulley
- Inertia limits
- Belts, contact length, and bearings
- Torques and speeds of the motors
- Control gains
- Maximum current and power limits of the amplifier

In this mechatronic system, both the mechanical design and the control design influence the overall system performance. The primary mechanical design decision is the diameter of the capstan pulley. The required line speed and machining tolerances are the basis of the design. When no disturbances are present, these determine the maximum possible variations in diameter.

The typical capstan drive is shown in Figure 4. Belt tension, damping, and bearing loads are present. The tension in the belt is significantly higher than the small tension in the fiber required to pull it (typically 50 to 100 grams tension). Dynamic effects of the capstan belt and bearings can be treated as viscous damping and additional inertia.

Although the belts are not the focus of this case study, they are an important part of the design. The belt material, contact length, and belt tension must be selected appropriately to achieve non-slip belt movement with respect to the capstan pulley. The belt/capstan friction and prevention of fiber coating damage are other key considerations.

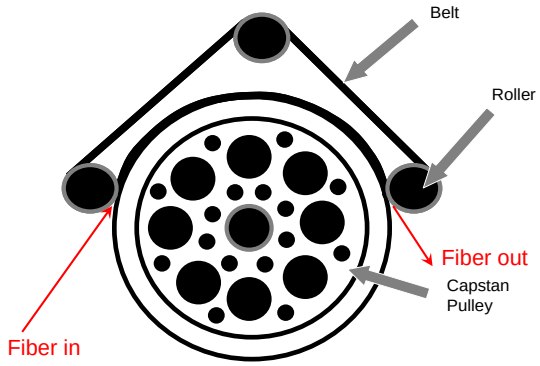

Figure 4. Capstan pulley with belt with three rollers

Capstan drives with smaller diameters are preferred. In addition to a lower mass moment of inertia and faster dynamic response with less control effort, they have less material and lower machining costs. The diameter of the capstan pulley is limited on the lower end by the mechanical strength of the fiber under tension and bending. Experiments have shown that the smallest allowable diameter is 75 mm. The diameter selection must also consider machining tolerances and maximum motor speeds. Half of the design error (0.05%) is budgeted to the mechanical tolerances, while the other half is allocated to the control design. Potential machining tolerances of ±0.05 mm on the diameter indicate that a diameter of 100 mm or larger must be used to meet the maximum design error, as seen in Figure 5. The mass moment of inertia of the capstan pulley is a parabolic function of diameter as seen in Figure 6. The lower the pulley inertia, the smaller the required control effort and power. As such, smaller diameter pulleys are more desirable given the control and inertia effects.

Another important consideration in the capstan design is the maximum speed of the motor. To allow for diameter control at a normal draw line speed of 50 m/s, the maximum line speed must be higher. Figure 7 depicts the relationship between motor

RPM and pulley diameter for an operational draw line speed of 60 m/s. Based on speed requirements, two potential diameters are possible. For a motor with a limit of 4,000 RPM a pulley diameter of approximately 300 mm (or larger) is required. A pulley diameter of about 200 mm is the minimum necessary diameter for a 6,000 RPM limit. With previously established design preferences for smaller diameter pulleys, the 200 mm diameter pulley is the logical choice if a motor with a maximum speed of 6,000 RPM or greater is available and meets the electrical requirements.

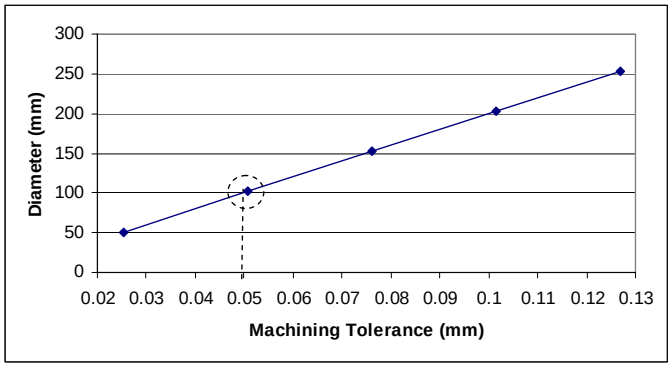

Figure 5. Pulley diameter vs. machining tolerance for 0.05% radius variation

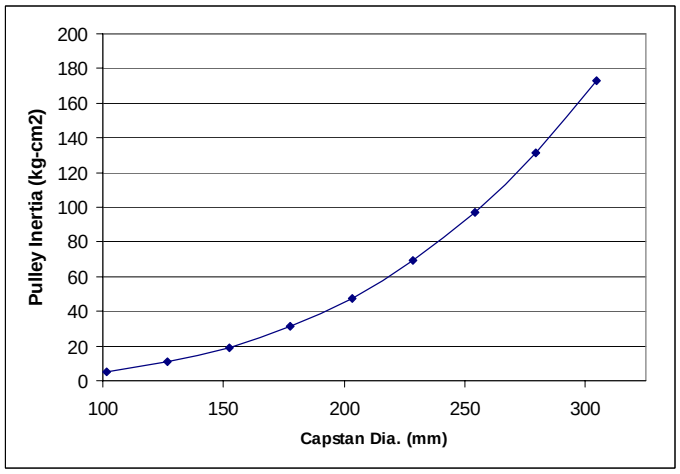

Figure 6. Capstan pulley inertia vs. diameter

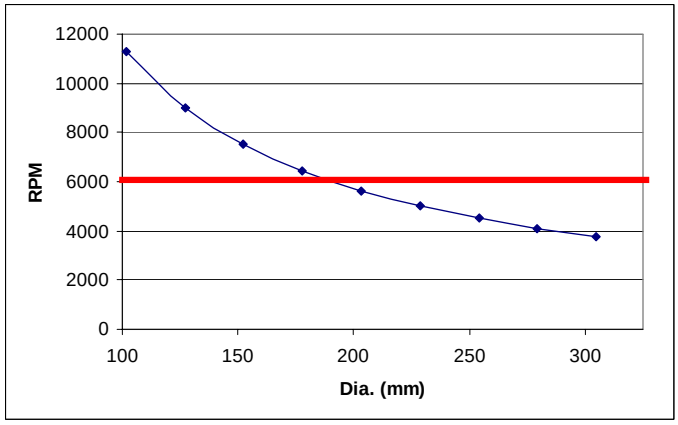

Figure 7. Motor RPM vs. pulley diameter for 60 m/s line speed

MOTOR SELECTION

A motor can be selected for each of the two possible diameters (200 mm and 300 mm) of the capstan pulley. The choice of motor depends on several factors including maximum speed, torque, inertia, current, and power limitations. The motor must handle the controller amplifier power limits of 800W per axis continuous and 1600W peak. The rated motor current must be greater than the maximum amplifier current of 10A to prevent overheating. Specifications for motors compatible with the specified controller and amplifier are presented in Table 1. The most distinguishing parameters for the listed motors are maximum speed and torque constants. Current and power limits are generally affected by accelerations of line speed. Given the amplifier limits, most of the motors will not approach their current and power limitations during operation at line speed.

From Table 1, motors 3, 5, or 7 achieve the speed (6,000 RPM), power, and current requirements for a 200 mm diameter pulley. Motor 3 is selected because of its relatively lower rotor inertia and approximately equivalent torque constant. For the 300 mm diameter pulley design, a motor rated at 4,000 RPM or higher is required. Motors 4 or 10 would be acceptable. While motor 4 is slightly below the maximum current limit specification (9.6 A), it has a 20% higher torque constant in comparison to motor 10. Thus, there are two potential candidate capstan designs: a 200 mm diameter pulley with motor 3 or a 300 mm diameter pulley with motor 4. The capstan design with the smaller pulley (200 mm diameter) is preferred.

Table 1. Specifications for Available Motors [7]

Model	Motor	Rated Power (kW)	Rated Torque (N-m)	Rated Speed (RPM)	Torque Constant (N-m/A)	Rated Current (Amps)	Rotor Inertia (kg cm2)
ASM121A-5	1	1.75	2.2	4,000	0.5	5	5.7
ASM121A-22	2	2.555	2.2	6,000	0.3	7.3	5.7
ASM121B-11	3	4.97	4.4	6,000	0.31	14.2	9.9
ASM121B-16	4	3.36	4.4	4,000	0.46	9.6	9.9
ASM121C-7	5	7.7	6.6	6,000	0.3	22	12.9
ASM121C-14	6	3.85	6.6	3,000	0.6	11	12.9
ASM143A-08	7	11.2	9.2	6,000	0.29	32	22
ASM143A-14	8	6.23	9.2	3,000	0.52	17.8	22
ASM143A-16	9	5.25	9.2	3,000	0.62	15	22
ASM143A-40	10	8.155	9.2	4,000	0.39	23.3	22

DERIVATION OF DYNAMIC EQUATIONS OF MOTION

The dynamic equations of motion for the capstan pulley system are developed using the parameters depicted in Figure 8.

$$\sum T(t) = J_{total}\ \dot{\omega} \tag{1}$$

or

$$J_{total}\dot{\omega} = -B_{total}\omega + T_{motor} \tag{2}$$

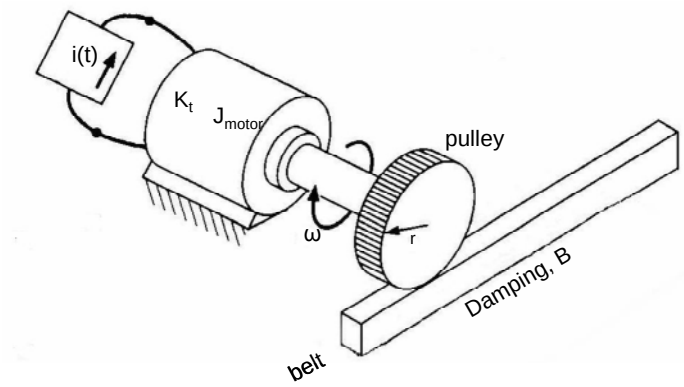

Figure 8. Idealized optical fiber draw capstan pulley (adapted from [9])

The motor torque is a function of the applied current.

$$T_{motor} = K_t i(t) \tag{3}$$

Substituting Eq. 3 into Eq. 1 yields Eq. 4.

$$J_{total}\dot{\omega} = -B_{total}\omega + K_t i(t) \tag{4}$$

The effective mass moment of inertia about the capstan rotation center is the sum of the inertia of the motor rotor, pulley, belt and rollers.

$$J_{total} = J_{motor} + J_{pulley} + J_{belt} + J_{rollers} \tag{5}$$

The capstan pulley can be modeled as a rim and a flange.

$$J_{pulley} \cong M_{rim}r^2 + \frac{1}{2}M_{flange}(r-2\tau)^2 \tag{6}$$

The mass moment of inertia for the belt and three rollers is expressed in Eq. 7.

$$J_{belt} + J_{rollers} = M_{belt}r^2 + 3\left(\frac{1}{2}M_{roller}r_{roller}{}^2\right) \tag{7}$$

The effective damping of the system is the sum of the damping from the bearings and belt.

$$B_{total} = B_{belt} + B_{bearings} \tag{8}$$

Damping is difficult to calculate but can be estimated by input-output relationships. Reformulating Eq. 4

$$\dot{\omega} + \frac{B_{total}}{J_{total}}\omega = \frac{K_t}{J_{total}}i(t) \tag{9}$$

Taking the Laplace transform of Eq. 9 with no initial conditions

$$s\Omega(s) + \frac{B_{total}}{J_{total}}\Omega(s) = \frac{K_t}{J_{total}}I(s) \tag{10}$$

From Eq. 10, the transfer function between speed and current may be derived

$$G_M(s) = \frac{\Omega(s)}{I(s)} = \frac{\frac{K_t}{J_{total}}}{s + \frac{B_{total}}{J_{total}}} \tag{11}$$

Using Eq. 11, the total damping (Eq. 8) may be estimated from a current step input and velocity data via system identification tools [8]. The root of the first order system of the Eq. 11 is real and negative. Because damping values are typically small, the response of the motor may be relatively slow. Control will be necessary for effective disturbance rejection.

CONTROL DESIGN AND PARAMETERS

The block diagram in Figure 9 represents a scheme for the diameter and speed control of the draw capstan. The approach taken here is a cascaded controller of an outer fiber diameter control loop with an inner capstan speed control loop. Diameter error is used to change the capstan speed set point, based on constant volumetric flow. The volumetric flow rate is the square of the fiber diameter multiplied by the capstan pull speed and $\pi/4$. A positive diameter error requires a positive speed increase to lower the diameter. The motor speed change from the diameter variation is relatively small. The speed

change is added to the original speed set point. Thus, the fiber diameter control is fine tuning the velocity set point.

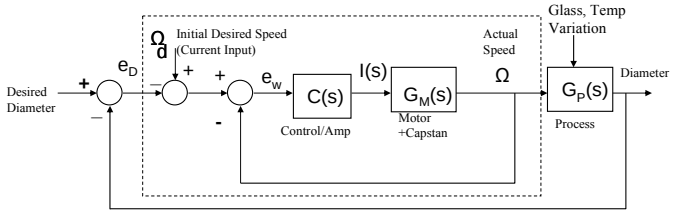

Figure 9. Capstan speed is controlled within a cascaded control loop for fiber diameter

The open-loop capstan speed transfer function, $G_M(s)$, is a first order system and yields an exponential function of time for a step change in current.

$$\omega(t) = \Delta I \left(\frac{K_t}{J_{total}} \right) \cdot \left[1 - e^{-\left(B_{total} / J_{total} \right) \cdot t} \right] \tag{12}$$

Although proportional control alone with a high gain can reduce the error, the steady-state error can be eliminated by using a compensator with proportional plus integral (PI) control.

$$C(s) = K_p \left(s + K_i / K_p \right) \tag{13}$$

In the creation of fiber the basic premise of capstan operation and speed control is constant volumetric glass flow, Q. The control logic is to increase the capstan speed set point if the fiber diameter is too thick or decrease it if it is too small. This is expressed in Eq. (14) and Eq. (15).

$$Q = \tfrac{\pi}{4} r \omega_d d_{act}^2 = \tfrac{\pi}{4} r \omega_{nom} d_{nom}^2 \tag{14}$$

$$\omega_d = \omega_{nom} \left(d_{nom} / d_{act} \right)^2 \tag{15}$$

Typical variations in the diameter of the glass preform can be approximated as a 2% change over 10 mm of the perform length. The shape assumed for the preform diameter deviation is a linear ramp. The ratio of preform diameter to fiber diameter is approximately 700:1. Squaring this gives a volumetric ratio of 490,000:1. Thus, the time for drawing 10 mm of preform (or 4900 m of fiber) would be approximately 100 s (fiber line speed of 50m/s). Squaring the diameter error yields a 4% volumetric variation over 10 mm of preform length. This volume error will be accommodated in the control design by changing the draw speed set point. Assuming a linear ramp function for the perform diameter (input), the line speed of the fiber would require a speed change ramp of 0.04% per second to keep the fiber diameter constant. In addition, this corresponds to 1.25 s for an uncontrolled fiber diameter to deviate to half of the tolerance budget (0.05% deviation). Thus, it is desirable to keep the settling time under one second for the inner speed loop to reduce the dynamic effects on the outer control loop.

CONTROLLER ELECTRICAL PARAMETERS

To ensure the capstan design performs as expected, it is necessary to identify the controller electrical specifications and verify they are not exceeded. Amplifier power is limited to 800 W per axis continuous and 1600 W peak. Current is limited to 10 A per axis. The controller maximum update rate is 20 kHz. With these performance specifications (summarized in Table 2) the capstan and controller design can be simulated. The selected 200 mm capstan pulley design with motor 3 can then be assessed.

Table 2. Summary of Controller/Amplifier Specifications for Capstan Axis

Maximum Power	1600 W peak; 800 W continuous
Maximum Current	10 A
Settling time	1.0 s or less
Sample rate	1 to 20 kHz

The open loop transfer function for the capstan pulley, motor, and speed controller is presented in Eq. 16. The speed controller, $C(s)$ was designed with PI feedback control.

$$C(s)G_M(s) = \frac{\Omega}{\Omega_d} = \frac{K_p \left(K_m / J_{total} \right) \left(s + K_i / K_p \right)}{s^2 + \left(B_{total} / J_{total} \right) s} \tag{16}$$

The integral and proportional gains, K_i and K_p, were determined using root loci and simulation techniques. An underdamped oscillatory speed response that can cause significant speed error must be avoided, so all roots for Eq. 16 were designed to be on the negative real axis. From a frequency domain perspective it was desirable to have a high ratio of integral to proportional gain. This was realized by placing the transmission zero farther along the negative real axis away from the origin. Values of 5 through 10 for the K_i/K_p ratio were determined effective through root locus design and verified through simulation. Stable values of K_p were found from 0.3 to 30. Figure 10 depicts typical continuous root loci for K_i/K_p=5. A non-oscillatory response can be achieved by keeping the system poles on the real axis.

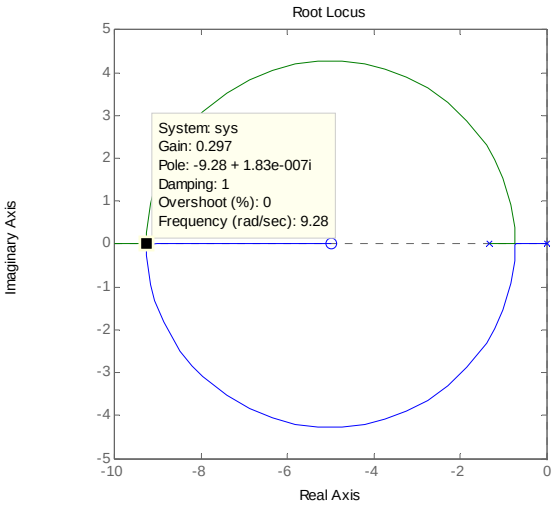

Figure 10. Continuous root loci

Another important controller design consideration is the digital root stability in the controller loop. As controller update rates range from 1 to 20 kHz, 1 kHz sampling was used to assess stability. The discrete model of the continuous system of Eq. 16, given by Eq. 17, was determined assuming a zero order hold on the input. A value 10 was assumed for K_i/K_p.

$$C(z)G_M(z) = \frac{K_P\left(0.03924z - 0.03885\right)}{z^2 - 1.9987z + 0.9987} \qquad (17)$$

Stability was found for values of proportional gain where a critical damped response was achieved (with values of 5 and 10 for the K_i/K_p). The design constraint of a non-oscillatory response was more limiting than discrete stability. Results for acceptable values of K_p from the discrete root locus design were found to be nearly identical to those obtained from the continuous root locus design due to the relatively fast sampling rate.

RESULTS

Simulation studies were performed with a Simulink™ model of the capstan speed control subsystem shown in Figure 11. Since fiber diameter is a function of the capstan speed, the velocity error may be directly related to the fiber diameter error (Eq. 14). A 4% ramp increase in the line speed set point over 100 s was modeled and simulated to represent the perform diameter input change. Line speed error, diameter error, and motor current were examined for various gains modeling the 200 mm capstan pulley and motor 3. The purpose of the simulation was to assess the capstan speed controller design with anticipated input.

Figure 12 depicts the results of four simulation cases for (a) K_p=30, K_i/K_p =5, (b) K_p=3, K_i/K_p =5, (c) K_p=0.3, K_i/K_p =5, (d) K_p=3, K_i/K_p =10. From these results the design with a 200 mm capstan pulley and motor 3 using K_p=3, K_i/K_p =10 meets the performance specifications. The settling time for speed was under 0.5 s while power and current limits were not exceeded. Given these favorable results, the gains of K_p = 3, K_i/K_p = 10 were selected as the final design gains for the speed controller.

The fiber diameter error shown is well within tolerances. However, it should be noted that the model does not include other processing variables as noted earlier, such as preform feed speed, furnace temperature, and measurement time delay.

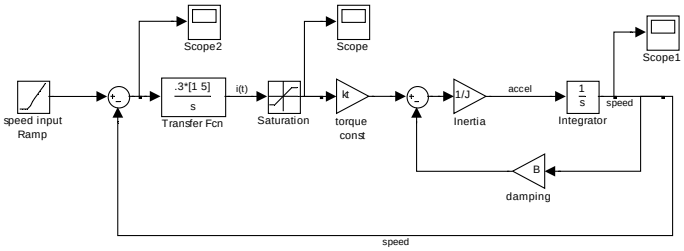

Figure 11 Simulink™ model of speed control loop

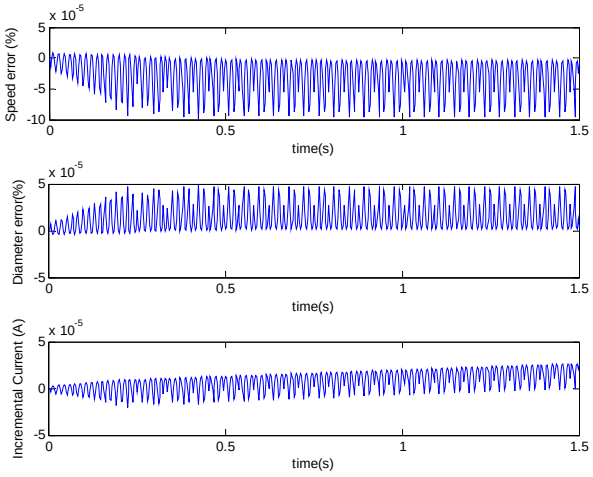

Figure 12(a). Simulation results: Line speed error and motor current for K_p=30, K_i/K_p =5

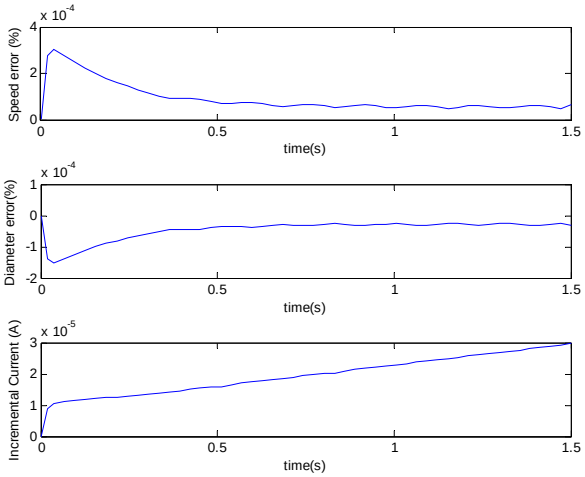

Figure 12(b). Simulation results: Line speed error and motor current for K_p=3, K_i/K_p =5

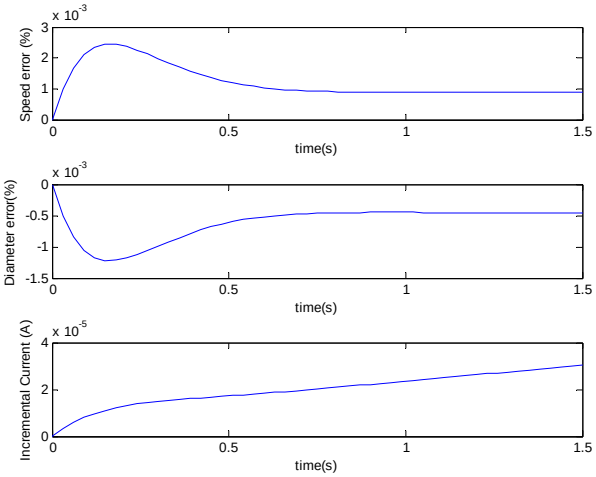

Figure 12(c). Simulation results: Line speed error and motor current for K_p=0.3, K_i/K_p =5

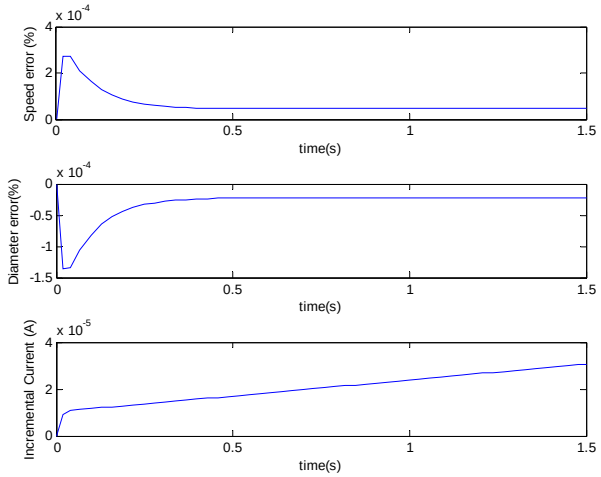

Figure 12(d). Simulation results: Line speed error and motor current for K_p=3, K_i/K_p =10

CLOSING

The design of an optical fiber draw capstan pulley including the motor selection and speed control system has been demonstrated for improved optical fiber diameter control. A stable, exponential response was achieved, without current saturation, for capstan speed in the presence of estimated process disturbances. With the design and process relationships established, an effective draw capstan system was synthesized and controlled.

Through this example students can gain a fundamental understanding of the process of applying classroom theory to solve a real-world problem. There are several key steps in the design and development of the capstan system presented in this paper that are worthy of study. The modeling of the process and the selection of the design parameters using multi-disciplinary criteria were used to develop a machine that performed better than that possible by serial (i.e., sequential) design.

Although specific hardware and software systems change, the fundamental engineering science underlying the successful design of a device, machine, or process has remained relatively constant. From this case study students can observe an effective approach for machine design and process control that relies on modeling, analysis, and simulation. A successful method of design with simulation was built upon (1) problem definition, (2) determination of parameters that affect control, (3) system model techniques, (4) physical and power limitations, (5) frequency domain control design, and (6) discrete control design. Due to its multi-disciplinary nature, this design case study has broad applications to practical engineering including control, electrical, and mechanical systems, typical in modern manufacturing.

REFERENCES

[1] Auslander, D. M., "What is Mechatronics?" *IEEE Transactions on Mechatronics*, Vol. 1, No. 1, 1996.

[2] Panaitescu, R., "Improving machine designs with mechatronics," *Design News*, September 25, 2006.

[3] Jenkins, H.E. and Nagurka, M.L., "Teaching a Senior-Level Mechatronics Course in Mechanical Engineering," *2004 Japan-USA Symposium on Flexible Automation*, Denver, CO, paper UL-047, 2004, pp.1-7.

[4] Refi, J., *Fiber Optic Cable: A Light Guide,* ABC Teletraining, Geneva, IL, 1991.

[5] Li, T. (Ed.), *Optical Fiber Communications*, Vol. 1, Academic Press, Inc., Orlando, FL, 1985.

[6] MacChesney, J.B., O'Connor, P.B., and Presby, H. M., "New Technique for the Preparation of Low-Loss and Graded Index Optical Fibers," *Proc. IEEE*, Vol. 62, No. 9, 1974, pp. 1282-3.

[7] URL:http://www.berkeleyprocess.com

[8] Ljung, L., *System Identification: Theory for the User*, Prentice Hall, Englewood Cliffs, NJ, 1987.

[9] Shearer, J.L., Kulakowski, B.T. and Gardner, J.F., *Dynamic Modeling and Control of Engineering Systems*, Second ed., Prentice-Hall, 1997, p.219.